Eur. Phys. J. B **45**, 63–68 (2005)
DOI: 10.1140/epjb/e2005-00165-8

THE EUROPEAN PHYSICAL JOURNAL B

Frequency dependent electrical properties of nano-CdS/Ag junctions

D. Mohanta[a] and A. Choudhury

Department of Physics, Tezpur University, P.O. Napaam, Assam-784 028, India

Received 18 October 2004 / Received in final form 16 February 2005
Published online 16 June 2005 –

Abstract. Polymer embedded cadmium sulfide nanoparticles/quantum dots were synthesized by a chemical route using polyvinyl alcohol (lmw) as the desired matrix. In an attempt to measure the electrical properties of nano-CdS/Ag samples, we propose that contribution from surface traps are mainly responsible in determining the $I{\sim}V$ and $C{\sim}V$ characteristics in high frequency ranges. To be specific, beyond 1.2 MHz, the carrier injection from the trap centers of the embedded quantum dots is ensured by large current establishment even at negative biasing condition of the junction. The unexpected nonlinear signature of $C{\sim}V$ response is believed to be due to the fact that while trying to follow very high signal frequency (at least 10^{-3} of recombination frequency), there is complete abruptness in carrier trapping (charging) or/and detrapping (decay) in a given CdS nanoparticle assembly. The frequency dependent unique role of the trap carriers certainly find application in nanoelectronic devices at a desirable frequency of operation.

PACS. 81.05.Dz II-VI semiconductors – 82.45.Yz Nanostructured materials in electrochemistry – 73.63.Kv Quantum dots – 73.21.La Quantum dots

1 Introduction

Over the years, research in nanoparticles, nanophase and nanocomposites have received prime interest due to size dependent tunable electric, magnetic and optoelectronic properties [1–3]. Amongst II-VI wide and direct energy-gap semiconducting compound materials, CdS is the most popular system due to simplicity for large scale production and relatively large exciton binding energy. Ever since it became possible to make nanocrystals of such polar semiconductor, there is extensive literature available with regard to spectroscopic and luminescence aspects [4–6]. The role of interfacial charge transfer have been reported in systems in which the CdS nanocrystal is either capped or coupled with a different wide band gap semiconductor system [7–9]. Soliman et al. have investigated morphological, structural and optical properties of polycrystalline CdS as a function of various dopant concentrations (Al, Cu, Fe etc.) [10]. Moreover, they claim incorporation of doping leads to formation of nanostructure phase in CdS films. Normally, due to size quantization, blueshift in the onset of absorption and exciton absorption are noticeable in the optical absorption spectra. Resonant Raman spectroscopy is helpful in identifying surface phonons which could be detectable in the low frequency wing of the LO mode [11,12]. Although effort has been put in $CdS_{1-x}Te_x$ system to investigate electrical transport properties with application possibility in electrochemical conversion [13], there is hardly any report available for such a widely investigated system with specific emphasis in frequency dependency. In this report, we present frequency dependent electrical properties of nano-CdS/Ag system by studying $I{\sim}V$ and $C{\sim}V$ characteristics across different ranges of frequencies. Also, we highlight expected application of such nano-CdS/Ag junctions.

2 Experimental

First, a rigid and atactic polymer namely, polyvinyl alcohol (PVA) was chosen as the matrix for embedding nanoparticles. Introducing cadmium metal ions into the ligands of the polymeric chain followed by hydrogen sulfide gas treatment led to the growth of cadmium sulfide nanoparticles embedded in the polymer matrix. The cadmium sulfide nanoparticle samples are casted on laboratory glass slides, dried in vacuum oven and then washed with ammonia. The process was repeated thrice and finally kept overnight for natural drying. The fabrication details has been reported elsewhere [14]. Next, thick nanoparticle embedded polymer film was removed from the substrate and kept ready for subsequent experimentations. Also, polymer film without nanoparticles was preserved as reference.

We have chosen 1.21 μm thick CdS/PVA films for investigation. They were shaped into a diameter of 8.3 mm (size of the holding plates). Schottky junctions were fabricated by means of thin Ag coating and the samples

[a] e-mail: best@tezu.ernet.in

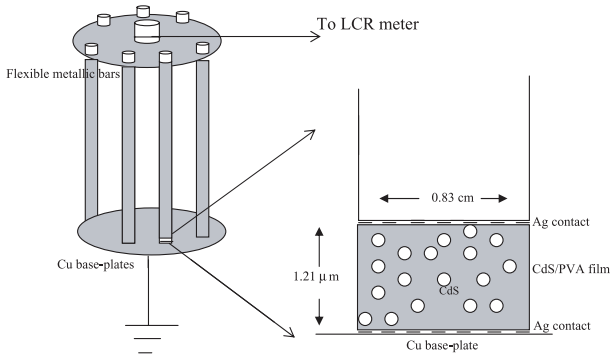

Fig. 1. Schematic of nano-CdS/Ag junctions for $I \sim V$ and $C \sim V$ measurements.

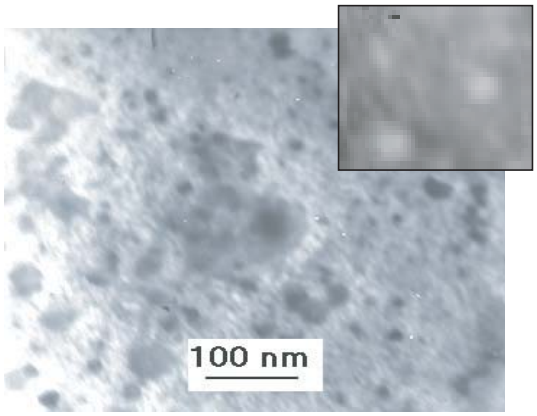

Fig. 2. TEM image of polymer embedded CdS nanoparticles.

were placed in a specially designed flexible sample holder (Fig. 1). The contact leads were taken from upper and lower plates by means of copper wires. Since ours is not a case of real CdS/Ag contacts, reverse biasing showed only minimal current growth ($\sim\mu$A/m^2) and therefore, only forwardly biased comparative $I\sim V$ measurements were carried out by using Hioki 3532-50 LCR Hi-Tester through 50–700 Hz, 1.0–50 KHz and 1.2–5.0 MHz series of frequencies. Also, Capacitance-Voltage ($C \sim V$) measurements were carried out by using the same variable frequency LCR meter and at experimental condition 293 K.

3 Results and discussion

Transmission electron microscopy (TEM) provides visible information regarding nanoscaled materials. Figure 2 represents a bright field TEM image of CdS nanoparticles embedded in the polymer matrix. Essentially, isolated and spherical nanoparticles within a size range 2–7 nm were observable, which is indicated in the figure-inset.

The $I \sim V$ characteristics of a typical solid state junction determines its working condition governed by the role of charge carriers and the barrier. Schottky contacts are metal-semiconductor junctions which are valuable when high speed rectification is required where as ohmic contacts are useful for non-rectifying operations. It was known that bulk-CdS/metal junctions drives current relatively at higher bias voltage with respect to nano-CdS/metal junctions [15]. Here we made an extensive study on nano-CdS/Ag junctions at three different frequency ranges viz. low (50–700 Hz), medium (1–50 KHz) and high (1.2–5 MHz), respectively. We discuss them independently.

3.1 Low frequency behaviour (50–700 Hz)

It was repeatedly observed that in the low frequency range, the current density ($J = I/A$) assumes a constant value i.e, $\sim$150.41 A/m^2. Moreover, J was found to be unchanged on increasing signal frequency across 50–700 Hz, even when the applied bias voltage was raised to 5.0 V.

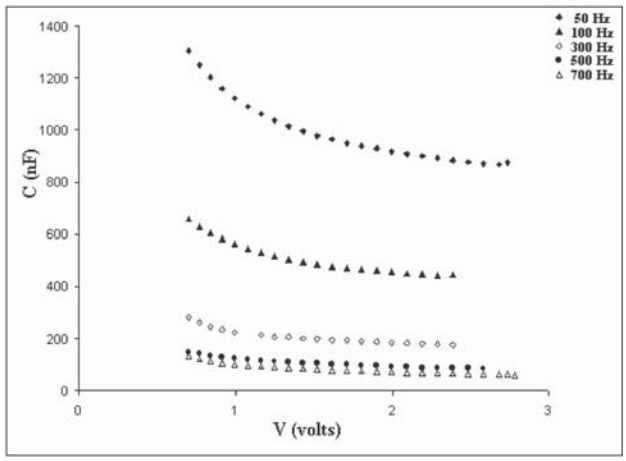

Fig. 3. $C \sim V$ response of nano-CdS/Ag junction (50–700 Hz).

We believe that this current could be due to incorporation of a finite carrier concentration as a result of Ag-diffusion. It is worthwhile to mention here that the diffusion coefficient (D_0) of the Ag ions in dilute aqueous solution is 10^{-5} cm^2/s at 298 K. Similarly, D_0 values through pure bulk CdS are 2.5×10^1 cm^2/s and 2.4×10^{-1} cm^2/s for slow and fast diffusions, respectively [16]. Thus, adequate electron concentration can be made available for sustaining current as Ag diffuses slowly into nano-CdS/PVA sample.

Figure 3 depicts $C\sim V$ plot in the low frequency regime. Earlier it was reported that with decrease in applied voltage, capacitance of the nano-CdS/Au junction steeply increases for a particular signal frequency [15]. In our nano-CdS/Ag system it has been found that as frequency increases from 50 Hz to 700 Hz the steepness of $C\sim V$ plot drops by substantial amounts. Such a nature can be explained by the fact that as Ag diffuses into CdS, electrons are loaded under biasing thus increasing the junction capacitance as a result of charging. Maximum charging effect is realized when almost no carriers respond to signal frequency (i.e. $\sim$50 Hz). Conversely, when frequency enhancement occurs a proportionate number of electrons would try to follow the signal frequency before being loaded into nano-CdS as a result of which junction capacitance drops down. Similarly, for a constant

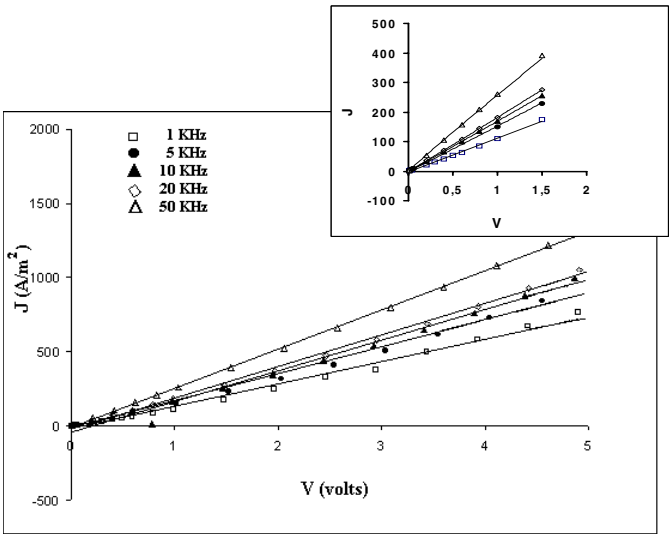

Fig. 4. $I \sim V$ response of nano-CdS/Ag junction (1–50 KHz).

signal frequency, if the bias voltage increases the loaded electrons would participate in current establishment and hence capacitance decreases considerably. But the extent of steepness of $C{\sim}V$ response falls with frequency and capacitance is likely to be uninfluenced for a maximum frequency (i.e. 700 Hz) when bias voltage was varied between 1–5 V. It is important to note that though $C{\sim}V$ response is strongly influenced by loading of electrons, the current establishment is still unchanged. Therefore, as a consequence of low frequency behaviour it is not the trapped carriers but the electrons loaded as a result of diffusion is mainly responsible for current conduction in the nano-CdS sample.

3.2 Mid-frequency behaviour (1–50 KHz)

The Figure 4 represents characteristic $I{\sim}V$ response of nano-CdS/Ag in the regime 1–50 KHz. The mid-frequency $I \sim V$ response highlights that the rate of forward current establishment (slope) increases uniformly with increase in signal frequencies. The inset shows response in the low bias regime, reverse biasing showed extremely low current ($\sim\mu$A/m^2, not shown). It is expected that CdS quantum dots which contain trapped carriers while trying to follow a.c. signal provide conducting channels through the sample giving rise to current establishment. Large becomes the signal frequency, more would be the no. of carriers participate for current establishment by dislodging themselves from the trapped centers (surface states). Although current-rate trend is quite uniform with respect to applied signal frequencies, current develops for voltage minima 127.52, 62.6, 200.95, 129.86 and 31.63 mV corresponding to frequencies 1, 5, 10, 20 and 50 KHz, respectively. Please note that these built-in potentials are estimated by fitting the trend lines to an accuracy of $\pm 0.001\%$. The rate of current growth is maximum i.e., 263.2 Ohm/m^2 at an applied voltage 31.6 mV and working signal frequency 50 KHz (Tab. 1). The applied voltage corresponding to rapid increase of current is showing oscillatory nature possibly due to adequate inhomogeneity in the quantum dots.

In fact, charge transport in PVA encapsulated CdS/Ag system can be explained by a similar mechanism as proposed by Greenham for CdS and CdSe nanoparticles embedded in a conjugated polymer MEH-PPV [17]. It was suggested that an electron-hole pair gets rapidly separated with electrons attracted towards the nanoparticles and holes on the polymer. Charge transport is then possible through nanoparticles and the polymer separately. A similar carrier transport was studied in CdS/porous silicon heterojunctions [18]. In this system, very high forward current densities so observed in the forward $I \sim V$ characteristics are attributed to the large interface of CdS/polymer on account of its proper integration with CdS quantum dots and the built in potential across the CdS/Ag nanojunction. In such a device, one has to ensure whether a tunneling [$I \propto V^2 \exp(a/V)$], thermionic [$I \propto \exp(-eV/nkT)$] or trap related [$I \propto V^m$] current model would come to the forefront [19,20]. We speculate that the third type model would be relevant to our case as linear current growth response indicates faster charge decay of the nanoparticles when signal frequency rises considerably. We estimated the characteristic value of the ideality factor (m) to be 0.95 to 1.05. It is absolutely important to note that such a situation cannot be due to ohmic-like characteristics as m purely depends on the trapped carrier concentration. An ideality factor exceeding 2 has been often found with nanostructure Schottky devices where the interface layer is an oxide [21].

It has been mentioned that the diffusion coefficient (D_0) of the Ag ions in dilute aqueous solution is 10^{-5} cm^2/s at 298 K and D_0 values through bulk CdS are 2.5×10^1 cm^2/s and 2.4×10^{-1} cm^2/s for slow and fast diffusions, respectively. Had the film been completely made of CdS, ions upon Ag coating would have diffused properly through the film within no time. Therefore, in such cases the role of trapped carriers is insignificant. Conversely, when CdS nanoparticles are embedded into a rigid and atactic matrix like polyvinyl alcohol complete diffusion is restricted by the matrix allowing isolated nanoparticles to respond in a unique way.

The Figure 5 represents $C \sim V$ response of the CdS quantum dot sample for mid-frequency range (1–50 KHz). It is predicted that contrary to the result shown by low range frequency values, capacitance increases enormously with applied voltage. However, the rate of increment drops when frequency improves and tends towards saturation at higher frequencies. For 1 KHz, capacitance attains highest value due to significant charging of the nano-CdS and that is why sustain least value of current (Fig. 4, Tab. 1) with respect to the cases of higher frequencies. PVA embedded CdS nanoparticles collectively behave as a capacitor to store charge, suppressing the chances of charge flow (current) from one terminal to the other. In fact, (i) for higher forward bias, there is large contributions from high density of surface/interface traps, and (ii) for low bias values, imply only a small contribution from surface traps. A high density of surface traps may lead to injection of minority carriers into the neutral zone, which in turn gives additional diffusion capacitance besides the normal depletion

Table 1.

Frequency f (KHz)	Rate of current growth $(\mathrm{d}I/\mathrm{d}V)/\mathrm{A}$ $(\mathrm{Mho/m^2})$	Applied voltage (Point of sharpest rise in current) (mV)
1.0	151.21	127.52
5.0	181.58	62.61
10.0	206.62	200.95
20.0	213.07	129.86
50.0	263.2	31.63

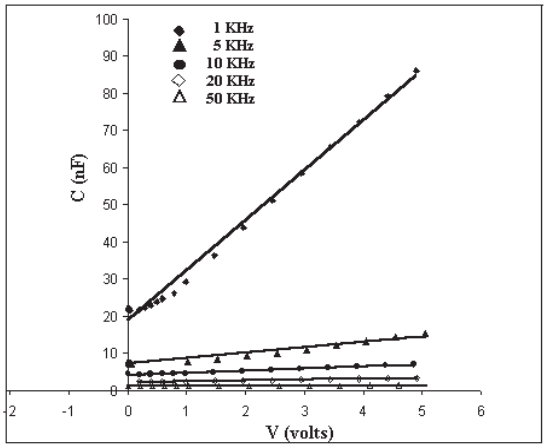

Fig. 5. $C \sim V$ response of nano-CdS/Ag junction (1–50 KHz).

layer contribution. Thus, the junction capacitance can be written as

$$C_j = C_{dep} + C_{diff} \ . \tag{1}$$

Further, the rearrangement of these injected minority carriers do not take place instantaneously and also become frequency dependent. For frequencies above the characteristic frequency of the recombination processes, these injected excess minority carriers are able to follow the a.c. signal and the C_{diff} contribution to C_j is mainly from the depletion layer. Since carrier recombination rate is of the order of $\tau \sim 10^{-9}$ s (equivalent to 1000 MHz), our experimental condition would not permit to sweep out all the trapped carriers from the nano-CdS. However, slight variation in a.c. signal frequency would definitely affect the nature of current establishment due to an ensemble of quantum dots. At higher frequencies, C_j attains saturation implying that the domain contribution to C_j is mainly from the depletion layer. The overall feature requires a frequency dispersion relation. Mott-Schottky hetero nanojunctions have been reported in case of metal-superconductor-semiconductors [22]. With experimental frequency variations within 1–15 KHz, the frequency dispersion discussed through the Mott-Schottky relation for a nano-CdS/Au junction given by [15]

$$\frac{1}{C_{dep}^2} = \frac{2}{q\varepsilon_0\varepsilon_s n_d}(V + V_{bi}) \tag{2}$$

where the quantities ε_0, ε_s, n_d, V_{bi} and C_{dep} are permitivity of the free space, the dielectric constant of the semiconductor, the donor concentration (CdS is an n-type semiconductor), the built in potential and the depletion layer

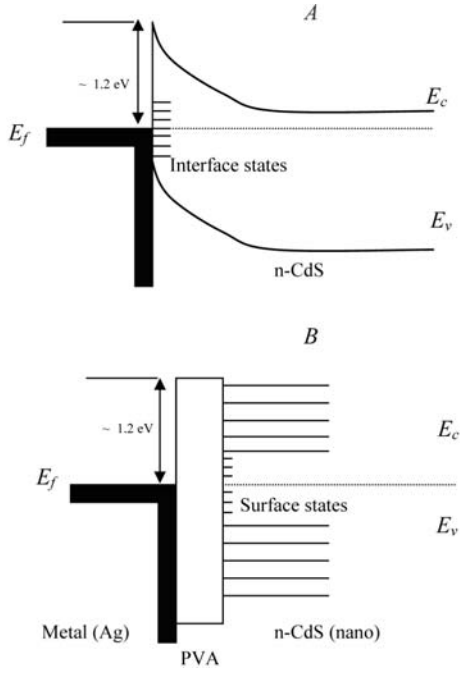

Fig. 6. Schematic of energy band profile for A) Ag/bulk CdS and B) Ag/nano-CdS

capacitance, respectively. Therefore, one can study Mott-Schottky response ($1/C_{dep}^2$ vs. V) to obtain built in potentials. In our case, such relation might valid for low frequency regime where nature of $C{\sim}V$ response is similar to the reported work. However, they considered study of Au-CdS interface layer, where Au is an efficient hole injector. Our case is distinct in the sense that there does not exist such interfacial layer, rather a thin dielectric polymer separating Ag and nano-CdS do exist. The trap carriers are mobile under high frequency and can tunnel through the barrier. Therefore, a single frequency dispersion equation describing $C{\sim}V$ for low to extremely high frequencies can not exist. Conversely, one can illustrate the mechanism of trapped carriers by using concept of band diagram.

Referring to Figure 6, a semiconductor surface contains surface states due to incomplete covalent bonds and other effects, which can lead to charges at the metal-semiconductor interface [23]. Furthermore, the contact is seldom an atomically sharp discontinuity between the semiconductor crystal and the metal. There is typically a thin interfacial layer which is neither semiconductor nor metal, normally ignored in case of ideal contacts. Because of the surface states, the interfacial layer, it is difficult

Table 2.

Frequency f (MHz)	Rate of current growth $(\mathrm{d}I/\mathrm{d}V)/\mathrm{A}$ (Mho/m^2)	Applied voltage (Point of sharpest rise in current) (mV)
1.2	1063.8	0.372
1.5	1280	−0.106
2.2	1844.9	−0.975
2.4	2019	−0.318
3.5	2733.2	−1.587
4.2	2597.7	−2.216
5.0	2144.9	−3.276

to fabricate junctions with barriers near the ideal values predicted from the work functions of the two isolated materials. So, measured barrier heights are used in the device design. For example, a collection of interface states in the semiconductor band gap that pin the Fermi level at a fixed position, regardless of the metal used. A collection of interface states located $0.7 \sim 0.9$ eV below the conduction band pins E_f at the surface of n-type GaAs, and the Schottky barrier height is determined from this pinning effect rather than by the work function of the metal [23].

The schematic energy-gap diagram for Ag-CdS ($E_g \sim 2.4$ eV) is shown in Figure 6. Figure 6A represents profile of Ag/bulk-CdS where as Figure 6B that of Ag/PVA/nano-CdS. In addition to the existence of discrete energy levels, the uniqueness of the later case is that the surface states are not in direct touch with the metal and thus permanently belong to nano-CdS. Such states, where electrons are believed to be trapped are made available to respond when one applies high signal frequency. In ideal case, the discrete levels are supposed to be slanted due to biasing to facilitate carrier transport. Now when the frequency of recombination matches with the applied frequency, all the trap carriers are expected to be swept away. On the other hand, low frequency would have negligible or no effect upon the surface traps. That is why within KHz and a few MHz frequency ranges current transport due to trap related mechanism is significant. Secondly, nano-CdS possess discrete energy levels (Fig. 6B) which could be slanted under proper biasing to facilitate current transport. Hence, it was evident that trapped carriers are basically frequency dependent where as electron transport between slanted quantized levels through thin dielectric polymer depends on the biasing condition.

3.3 High frequency behaviour (1.2–5.0 MHz)

Investigations in the high frequency (1.2–5 MHz) region ensure that the current in the quantum dot Ag/CdS junctions shoots up at ∼0.372 mV corresponding to signal frequency $f = 1.2$ MHz (Fig. 7). The maximum current growth i.e., 2733.2 mho/m^2 is found to be established at $f = 3.5$ MHz whilst least rate was 1063.8 mho/m^2 for $f = 1.2$ MHz. Considering $I \propto V^m$, the ideality factor varies from $m = 0.95$ to 1.15. One important conclusion can be drawn from Table 2 that for MHz ranges, current establishment takes place even if the quantum dot sample is under negative potential difference. This confirms excessive carrier injection from the surface traps

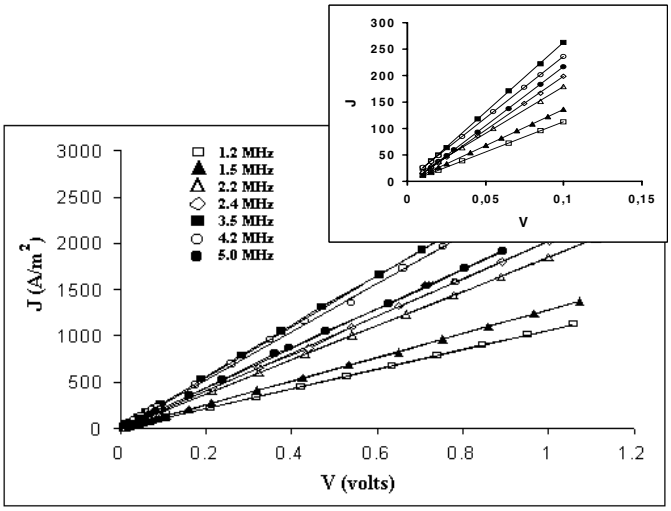

Fig. 7. $I \sim V$ response of nano-CdS/Ag junction (1.2–5.0 MHz).

plays dominant role in establishing current when one moves to high and higher frequencies. Figure 8 depicts $C{\sim}V$ characteristics in this regime which highlights great extent of nonlinear patterns. We believe this could be due to abrupt respond of the trapped carriers to very high applied frequency, even when they approach thousandth of the recombination frequency. Strong nonlinearity begins at $f = 2.4$ MHz and attains a maxima corresponding to $f = 4.2$ MHz. The inset of Figure 8 represents unique pattern of $C{\sim}V$ in the low biasing regime. It has been observed that charging (high capacitance) is faster at 1.2 MHz, which slows down for subsequently high frequencies. It is important to quote that observation of great extent of nonlinearity begins at ~ 0.1 V when there is simultaneous contribution from trapped carriers and carriers from slanted energy levels compete to follow signal frequency, which needs further investigation in this direction.

The nonlinear nature corresponding to charging and discharging process within a given range of forward bias for highly ordered quantum dots has been reported to find application in single electron devices, nano junction diodes etc. [24]. The nature of increase in conductance in heterojunctions due to photo-excitation has also been explored [25]. On the other hand, photon assisted tunneling in a single/arrayed quantum dot(s) is a recent issue which could find application in photonic switching and

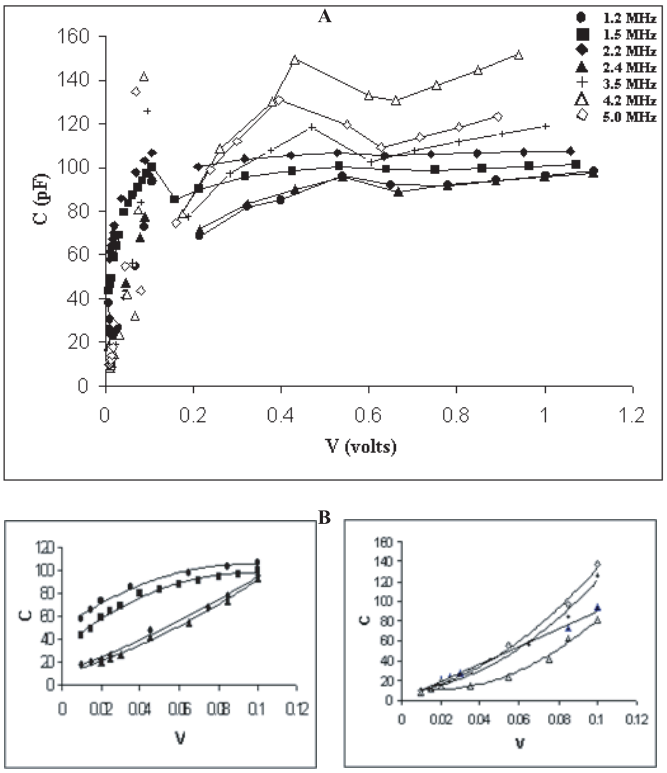

Fig. 8. A) $C-V$ response of nano-CdS/Ag junction (1.2–5 MHz) and B) that of low bias.

other optoelectronic devices [26,27]. Though our embedded nanoparticle system is a disordered one, formation of Schottky barrier is realized here at higher frequencies. Moreover, we have observed that for KHz and MHz ranges charging was possible even if applied voltage is of the order of a few millivolts only. Hence, embedded CdS quantum dots can be used as passive elements like capacitors etc. to justify the name of men made charge droplets in true sense. Moreover, the nature of trapped carriers controlled by signal frequencies would be a great asset to find application in nanoelectronics operated at selective frequencies.

4 Conclusion

Polymer embedded, spherical and isolated CdS nanoparticle formation was confirmed by TEM. Direct electrical probing of nanoparticles is a complicated and cumbersome task. Therefore, we attempted to explore electrical properties of nano-CdS/Ag at three different frequency ranges. We found that contribution of surface traps is mainly responsible in determining the nature of $I \sim V$ and $C \sim V$ responses at different ranges of frequencies. Current establishment even at the negative bias proves desired contribution from the trapped carriers at high frequencies. Hence, carrier transport due to such trap carriers controlled by signal frequencies can be suitably applied in nanoelectronics of desired working frequency.

The authors thank RSIC-NEHU, Shillong for providing TEM facility and ISRO, Bangalore for sponsoring the project. Also, the authors extend sincere thanks to the colleagues for valuable suggestions at various steps of the research work.

References

1. D. Meisel, P.V. Kamat, *Semiconductor Nanoclusters, Studies in Surface Sciences and Catalysis* **103**, 79 (1997)
2. A. Tilke, R.H. Blick, H. Lorentz, J. Appl. Phys. **90** (2), 9423 (2001)
3. P.M. Smowton, E.J. Pearce, H.C. Schneider, W.W. Chow, M. Hopkinson, Appl. Phys. Lett. **81** (17), 3251 (2002)
4. A. Balandin, K.L. Wang, N. Kouklin, S. Bandyopadhyay, Appl. Phys. Lett. **76** (2), 137 (2000)
5. J.J. Shiang, S.H. Risbud, A.P. Alivisatos, J. Chem. Phys. **98** (11), 8432 (1993)
6. A.I. Ekimov, I.A. Kudryavtsev, M.G. Ivanov, Al.L. Efros, J. Lum. **46**, 83 (1990)
7. R. Vogel, P. Hoyer, H. Weller, J. Phys. Chem. **98**, 3183 (1994)
8. H. Gerischer, M. Lubke, J. Electro. Chem. Interfac. Electro. Chem. **204**, 225 (1986)
9. I. Bedja, P.V. Kamat, J. Phys. Chem. **99**, 9182 (1995)
10. L.I. Soliman, H.H. Afify, I.K. Battisha, Ind. J. Pure, Appl. Phys. **42**, 12 (2004)
11. K.K. Nanda, S.N. Sahu, Appl. Surf. Sci. **119**, 50 (1997)
12. D. Mohanta, G.A. Ahmed, A. Choudhury, Chinese J. Phys. **42**, 740 (2004)
13. V.B. Patil, D.S. Sutrave, G.S. Shahre, L.P. Deshmukh, Ind. J. Pure Appl. Phys. **39**, 184 (2001)
14. D. Mohanta, S.K. Dolui, A. Choudhury, Indian J. Phys. **75A** (1), 53 (2001)
15. S.N. Sahu, B. Patel, S.N. Behera, K.K. Nanda, Indian J. Phys. **74A** (2), 93 (2000)
16. D.R. Lide, *CRC handbook of chemistry and physics* (CRC Press, New York, 2000-2001), pp. **12** 113
17. N.C. Greenham, X. Peng, A.P. Alivisatos, Phys. Rev. B **54**, 17628 (1996)
18. N.V. Deshmukh, T.M. Bhave, A.S. Ethiraj, S.R. Sainkar, V. Ganeshan, S.V. Bhoraskar, S.K. Kulkarni, *Nanotechnology* **12**, 290 (2001)
19. M.C. Schlamp, P. Xiaogang, A.P. Alivisatos, J. App. Phys. **82**, 5837 (1997)
20. D. Braun, A.J. Heeger, Appl. Phys. Lett. **58**, 1981 (1982)
21. H.P. Maruska, F. Namavar, N.H. Kalkhoran, Appl. Phys. Lett. **61**, 1338 (1992)
22. D.D. Shivagan, P.M. Shirage, S.H. Pawar, Pramana, **58** (5, 6), 1183 (2002)
23. B.G. Streetman, S. Banerjee, *Solid state electronic devices* (Pearson Education Ltd. India, 2004), p. 226
24. H. Grabet, M.H. Devoret, *Single Charge Tunneling: Coulomb Blockade Phenomena in Nanostructures* (Plenum Press, London, (1992)
25. L. Kouwenhoven, *Transport of electron-waves and single-charges in semiconductor nanostructures*, Ph.D. thesis, Delft University of Technology, The Netherlands (1992)
26. T.H. Oosterkamp, *Artificial atoms and molecules*, Ph.D. thesis, Delft University of Technology, The Netherlands (1998)
27. D. Mohanta, A. Choudhury, Physica E **27** (1, 2), 176 (2005)